Iowa State University
Digital Repository

Retrospective Theses and Dissertations

Iowa State University Capstones, Theses and Dissertations

1972

Filament formation in bulk samples of amorphous chalogenide As55Te35Ge10

Ven-che Kao
Iowa State University

Follow this and additional works at: https://lib.dr.iastate.edu/rtd

Part of the Electrical and Electronics Commons

Recommended Citation

Kao, Ven-che, "Filament formation in bulk samples of amorphous chalogenide As55Te35Ge10 " (1972). *Retrospective Theses and Dissertations*. 5260.
https://lib.dr.iastate.edu/rtd/5260

This Dissertation is brought to you for free and open access by the Iowa State University Capstones, Theses and Dissertations at Iowa State University Digital Repository. It has been accepted for inclusion in Retrospective Theses and Dissertations by an authorized administrator of Iowa State University Digital Repository. For more information, please contact digirep@iastate.edu.

المنارة للاستشارات

www.manaraa.com

INFORMATION TO USERS

This dissertation was produced from a microfilm copy of the original document. While the most advanced technological means to photograph and reproduce this document have been used, the quality is heavily dependent upon the quality of the original submitted.

The following explanation of techniques is provided to help you understand markings or patterns which may appear on this reproduction.

1. The sign or "target" for pages apparently lacking from the document photographed is "Missing Page(s)". If it was possible to obtain the missing page(s) or section, they are spliced into the film along with adjacent pages. This may have necessitated cutting thru an image and duplicating adjacent pages to insure you complete continuity.

2. When an image on the film is obliterated with a large round black mark, it is an indication that the photographer suspected that the copy may have moved during exposure and thus cause a blurred image. You will find a good image of the page in the adjacent frame.

3. When a map, drawing or chart, etc., was part of the material being photographed the photographer followed a definite method in "sectioning" the material. It is customary to begin photoing at the upper left hand corner of a large sheet and to continue photoing from left to right in equal sections with a small overlap. If necessary, sectioning is continued again – beginning below the first row and continuing on until complete.

4. The majority of users indicate that the textual content is of greatest value, however, a somewhat higher quality reproduction could be made from "photographs" if essential to the understanding of the dissertation. Silver prints of "photographs" may be ordered at additional charge by writing the Order Department, giving the catalog number, title, author and specific pages you wish reproduced.

University Microfilms

300 North Zeeb Road
Ann Arbor, Michigan 48106

A Xerox Education Company

72-26,925

KAO, Ven-che, 1937-
FILAMENT FORMATION IN BULK SAMPLES OF
AMORPHOUS CHALCOGENIDE $As_{55}Te_{35}Ge_{10}$.

Iowa State University, Ph.D., 1972
Engineering, electrical

University Microfilms, A XEROX Company, Ann Arbor, Michigan

THIS DISSERTATION HAS BEEN MICROFILMED EXACTLY AS RECEIVED

Filament formation in bulk samples of amorphous

chalcogenide $As_{55}Te_{35}Ge_{10}$

by

Ven-che Kao

A Dissertation Submitted to the

Graduate Faculty in Partial Fulfillment of

The Requirements for the Degree of

DOCTOR OF PHILOSOPHY

Major: Electrical Engineering

Approved:

Signature was redacted for privacy.

In Charge of Major Work

Signature was redacted for privacy.

For the Major Department

Signature was redacted for privacy.

For the Graduate College

Iowa State University
Ames, Iowa

1972

PLEASE NOTE:

Some pages may have

indistinct print.

Filmed as received.

University Microfilms, A Xerox Education Company

TABLE OF CONTENTS

		Page
I.	INTRODUCTION	1
II.	LITERATURE REVIEW	4
III.	EXPERIMENTAL RESULTS	9
	A. Sample Preparation and Chromium Electrodes Coating	9
	B. Experimental Arrangement	11
	C. Experimental Results	14
IV.	THEORY	26
	A. The Basic Property of the Amorphous Chalcogenide	26
	B. Critical Field Intensity and Breakdown Temperature	31
	C. Voltage Characteristic Curve of Filament Formation	38
	D. Connection Between the Anode and Cathode Filaments	45
	E. Growth Rate of the Filaments	46
V.	CONCLUSION	49
VI.	BIBLIOGRAPHY	52
VII.	ACKNOWLEDGEMENTS	54

LIST OF FIGURES

		Page
Figure 1.	The As-Te-Ge phase diagram in atomic percentage	10
Figure 2.	A top view of a portion of the chromium coated sample surface	12
Figure 3.	Experimental arrangement	12
Figure 4.	The relationship between the applied voltage and delay time	16
Figure 5a.	The anode filament grown from the anode on the surface 526X	17
Figure 5b.	The cathode filament appeared on the surface after etched in No. 1 chemical solution; same sample as 5a	17
Figure 6.	The voltage drop in the voltage characteristic curve corresponds to a connection between the two filaments	19
Figure 7.	No connection between two filaments with different surface texture: it is in low resistivity state	20
Figure 8.	With 3.55 ma conducting current the growth rate of the cathode filament is increased; the sample was etched in No. 1 chemical solution 526X	22
Figure 9.	The average growth rate of the filaments	23
Figure 10.	Topography of the memory filamentary path, etched with No. 2 chemical solution 1,700X	24
Figure 11.	Thermodynamic properties of a glass	27
Figure 12.	Thermodynamic properties of a glass	28
Figure 13a.	The geometry of the device	32
Figure 13b.	A side view of a simplified geometry for field calculation	32
Figure 14.	No connection between the two filaments, in high resistance state 526X	
Figure 15.	Top view of the device during the filament formation	42

		Page
Figure 16.	Temperature and current density within slab at various times after the application of electric field $5.9X10^5$ V/cm	44
Figure 17.	Two connections between the two filaments, etched with No. 1 chemical solution for 1 sec. 526X	47

I. INTRODUCTION

Industrial semiconductor devices are primarily made from germanium and silicon crystals with impurity doping. The virgin crystals exhibit nearly perfect long range periodicity. In recent years considerable attention has been focused on the study of amorphous materials which lack long range periodicity. These materials can be made from low purity materials without disturbing their intrinsic properties. Some of the amorphous materials have shown the property of reversible bistable resistivity and some of the others have a threshold switching property (1, 2, 3). In the materials which have the bistable resistivity, the resistivity between two stable states differs by at least four orders of magnitude. Since the memory devices used in a computer have two distinguishable stable states, the amorphous materials with bistable resistivity have potential application in the field of computer memories.

The first thin film memory device made from the amorphous chalcogenide was reported by Ovshinsky (2) and Sie (3) separately in 1968. However, the memory filament formation associated with the memory switching was observed later in bulk samples of amorphous chalcogenide As-Te-Ge system in 1970 by Uttecht et al. (4). The memory filament grew from the anode in these samples. However, the filament grown on the top of the material did not completely form between the electrodes as reported. Since the filament formation between the electrodes will result in a switching from a high resistivity to a low resistivity state, the memory filament has to be completed in order to achieve a memory switching. The memory filament is also expected to be in a crystallized state (5, 6). In an attempt to

shed some light on the filament formation process in the amorphous chalcogenide and associated switching mechanism, this thesis reports some observations and some properties of the filament formation in surface switching on the bulk samples.

The amorphous chalcogenide $As_{55}Te_{35}Ge_{10}$ is chosen in this study because the memory filament formation is slow. The experiments are performed in normal atmosphere at room temperature. The application of a current limited voltage pulse across the electrodes results in a filament formation. The filaments are examined under an optical microscope. Chemical etching is used to expose the filaments which have been grown under the surface, and to etch away the surface layers of the filament in order to examine its structure by electron scanning microscopy. The composition of the memory filament is determined with an electron microprobe analyzer.

The most important result of this study demonstrates that there are two filaments formed in the memory switching process for the amorphous chalcogenide $As_{55}Te_{35}Ge_{10}$. One is initiated from the anode and the other from the cathode. For the geometry used the anode filament grows on the surface in this material and the cathode filament grows under the surface. The surface texture of both filaments are different. The manner of connection between the anode and the cathode filaments influences the length of the memory switching time.

During the filament formation the current is limited by a resistance in series with the voltage pulse generator and is maintained constant. It is further discovered that a sudden voltage drop in the voltage

characteristic curve (the relationship between the voltage across the electrodes vs time) of the memory filament formation corresponds to a connection between two filaments. Without a connection no sudden voltage drop in the curve is observed.

With a low conducting current the growth rate of the anode filament is relatively constant and faster than that of the cathode filament. The growth rate of the cathode filament can be increased by applying a higher conducting current. With increasing conducting current level, the growth rate of the memory filaments has a tendency to saturate.

II. LITERATURE REVIEW

In recent years considerable attention has been focused on the study of amorphous semiconductors, in particular the chalcogenides. The chalcogenide semiconductors are a class of the amorphous semiconductors which exhibit bistable resistivity (1). The physical process taking place after electrical breakdown sets the amorphous semiconductors apart from other dielectric materials in which a breakdown causes permanent damage. Memory and threshold effects may be observed in these types of materials because of their non-destructive property. Since the amorphous semiconductors only preserve a short range order of the structure, minute impurities and other defects are not important factors in determining their properties. They behave as intrinsic materials.

Ovshinsky (2) was the first to report the reversible switching of an amorphous thin film from an insulating state to a conducting state. Since then several theoretical models and experiments have been proposed and conducted to explain the switching mechanism in the amorphous semiconductors. Mott (7, 8) proposed that a sudden transition from an insulator to a conductor can be induced by applying an external high electric field. If sufficiently large, the electron wave-function on each atom will overlap with its neighbor and bands will be formed. The solid should immediately become a conductor. This should happen, however far apart the atoms might be. This is the so called Mott transition and the electronic mechanism is a dominate factor. He also pointed out that the amorphous semiconductors with widely varying valences behave as intrinsic materials because the individual atoms have their valence requirements

satisfied locally. Consequently, the potential energy varies from place to place without any periodic pattern as observed in the crystallized materials, and the mean free path of the carriers is considerably reduced. When the mean free path of the carriers is reduced to the order of the atomic distance, an energy eigenfunction of the carrier can only be expressed by summing the localized wave functions with random phase factors. In a crystallized material the energy eigenfunction can be described by a plane wave. Cohen, Fritzsche, and Ovshinsky (9), using some of Mott's ideas, proposed a model with overlapping of the band tails ---- the mobility gap model. According to them, the energy states of the conduction band in the mobility gap may not be necessarily higher than that of the valence band. The overlapping band tails creates very effective trapping centers when the conduction band states in the band tail are occupied and the valence band states are unoccupied. They proposed to use the mobility of the carriers to distingush the carriers with different transition mechanisms. Two well defined energies are used to describe the transition points of mobility (10). In between these two energies is the so called mobility gap, and in this gap the mobility is very low. The conduction process changes from a low mobility band transport with finite mobility at T = 0 deg. K to a thermally activated hopping between localized gap states which disappears at T = 0 deg. K.

Hindley (11) further developed a model with random phase factors in the summation of localized wave functions and calculated the energy transfer between electrons and phonons in a very high applied field. For the chalcogenide semiconductors the interaction between the electrons and

optical phonons becomes very strong in a high applied field in the order of 10^5 V/cm. It is felt that hot electrons play an important role in describing the switching mechanism in the chalcogenide semiconductors.

Boer (12) favored the extension of the solid state band theory by imposing a perturbation on both bands. The external high electric field reduces the potential barriers imposed on both bands. The electrons also will gain their kinetic energy from the applied field. The highly energetic electrons will cause conduction because of the tunneling effect. Mattis (13) succeeded in describing the insulator-metal transition by calculating the tunnel effect of the energetic carriers in a high applied field.

In 1968 Sie (3) reported the memory effect in the amorphous chalcogenide $As_{55}Te_{35}Ge_{10}$ thin film. Uttecht et al. (4) observed a filament growing from the anode to the cathode on the unpolished surface of the bulk chalcogenide samples by applying a D. C. voltage with hand controls in series with a load resistance. The slow growth rate of the filament in the amorphous chalcogenide $As_{55}Te_{35}Ge_{10}$ made it convenient to observe the growth phenomena and was shown in his cinematography movie. A higher applied voltage is needed to cause a breakdown in material of this composition compared to other composition in the same amorphous chalcogenide system. In most cases the surface filament was not completed between electrodes from Uttecht's direct observations. He proposed that the filament was grown underneath to connect the cathode. Two spring contact probes were used as electrodes in his experiment. The variation of the composition in the filament also was reported by Uttecht. Vaporized

species associated with the surface switching has been studies by Johnson et al. (14).

One finds that glasses can be heated up to a certain temperature and crystallization occurs with the releasing of latent thermal energy. If the supplied heat energy is controlled so that it does not cause the melting of crystallized material, the material will stay in the crystallized state after the termination of the heating. Since the process does involve a structure change from amorphous state to crystallization state, the material can be used as a memory material if it can be switched back to its initial amorphous state by another process. Fritzsche and Ovshinsky (15) confirmed the mentioned idea by measuring the differential thermal analysis of the amorphous chalcogenides. The amorphous chalcogenides which exhibit a memory effect have an exothermic transition temperature below the melting temperature. The exothermic transition temperature for As-Te-Ge chalcogenide system was studied extensively by Krebs and Fischer (6).

In 1969 Sie (16) reported a radiometric microscopy measurement of the growing filament on the surface of the bulk amorphous chalcogenide $As_{55}Te_{35}Ge_{10}$. After breakdown the apparent temperature between two electrodes reached 320 deg. C. This high temperature was maintained until the advancing filament passed through the spot where the radiometric microscope was used. The temperature in the filament was decreased to 32 deg. C.

Two kinds of mechanism have been suggested to explain the memory switching in the amorphous chalcogenides: an electronic mechanism and a

thermal mechanism. An equilibrium macrostate of a system can be characterized by its entropy where the entropy is a function of the characteristic parameters of the system. A thermal energy related change in the system parameters may result in an increase or a decrease in the entropy of the system.

Considering the electric field effect on the conductivity of the chalcogenide semiconductors, Warren and Male (17) calculated the thermal runaway. Warren's result (18) indicated that the thermal mechanism was a dominating factor for the switching. Kolomiets et al. (19) pointed out that it was an electronic mechanism governing the switching in the chalcogenide semiconductors because of the temperature insensitivity in their performance. Fritzsche and Ovshinsky (5) suggested that the thermal mechanism was dominant in the switching of a thick chalcogenide film (> 10 micrometers), while the electronic mechanism was dominant for a thin film switching.

III. EXPERIMENTAL RESULTS

A. Sample Preparation and Chromium Electrodes Coating

The glass formation region of the chalcogenide As-Te-Ge system is found in the work published by Hilton et al. (20). In this study $As_{55}Te_{35}Ge_{10}$ is chosen in the center of the right hand glass formation region in the phase diagram as shown in Figure 1. The As, Te, and Ge are weighed and placed in a quartz tube. The tube is evacuated with a mechanical pump and sealed with a hydrogen torch. The tube is placed in a rocking furnace at 980 deg. C. for 24 hours, lifted out of the furnace and quenched in air at room temperature in the horizontal position. The amount of $As_{55}Te_{35}Ge_{10}$ is about one-tenth of the total volume of the tube, and a fast cooling rate is obtained in the whole volume of the sample. The $As_{55}Te_{35}Ge_{10}$ samples are checked with electrical measurement and diffraction patterns. All measurements confirm that the experimental samples are good amorphous materials.

The bulk samples are mounted in plastic and polished by using fine sandpapers and 0.05 micrometer alumina calcined powder with a microcloth to obtain an optically flat surface. The polished samples are ultrasonically cleaned in a detergent solution and then degreased with isopropanol alcohol. A 4,000 Å chromium film is deposited through a mask onto the surface with an electron gun. A very slow deposition rate, 1 Å/sec., is used to make a good coating. A portion of a coated surface is shown in Figure 2. The chromium strips are 100 micrometers apart and are used as electrodes. Two spring contact tungsten carbide probes provide a

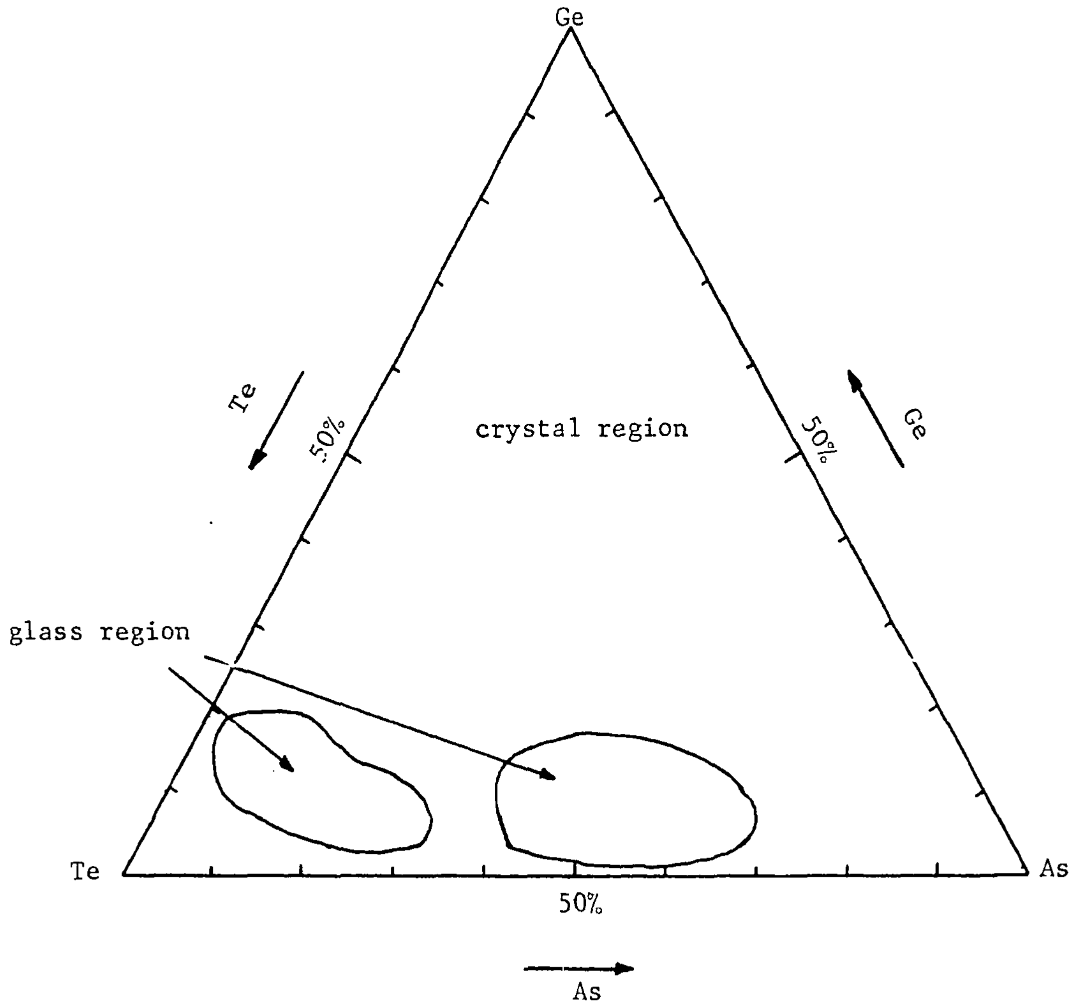

Figure 1. The As-Te-Ge phase diagram in atomic percentage (after Hilton)

connection between the chromium electrodes, pulse generators, and other equipments. There are several advantages to using chromium electrodes instead of two spring contact tungsten carbide probes:

1). better contact and adherence between the chromium electrodes and the amorphous chalcogenide is achieved before the memory filament is formed,

2). after the filament is formed, a better contact between the electrodes and the memory filament is achieved,

3). the stress in the amorphous chalcogenide around the probes area is reduced,

4). more reproducible data is achieved,

5). and finally the chromium electrodes have a high melting point and a very low oxidization rate in the atmosphere.

B. Experimental Arrangement

The diagram of the experimental arrangement for the switching of the amorphous chalcogenide devices is shown in Figure 3. For the first switch from an initial high resistivity state to a low resistivity state, a high voltage pulse with amplitude 180 volts and 7.6 seconds duration is applied across the chromium electrodes in series with a load resistor which limits the conducting current. In this study the value of the conducting current ranges from 1.8-3 milliamperes. To switch back to a high resistivity state, a 15-20 milliamperes, 5 microsecond duration pulse is applied across the filament in series with a load resistor of 1 kilohm. The amplitude of the pulse is 30-40 volts. The fall time of the current pulse

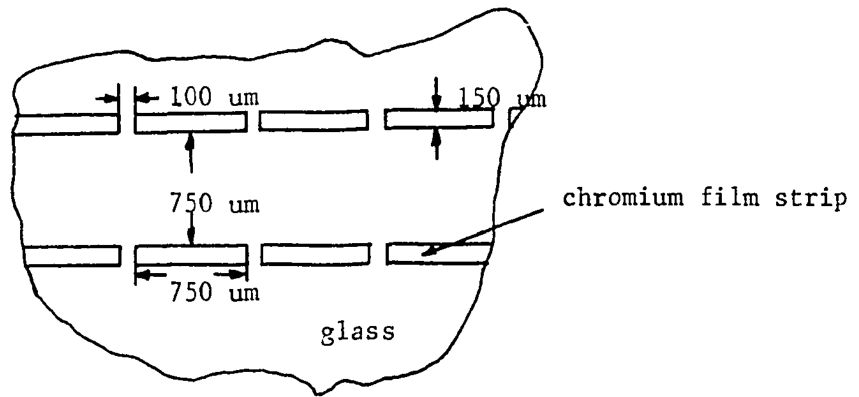

Figure 2. A top view of a portion of the chromium coated sample surface

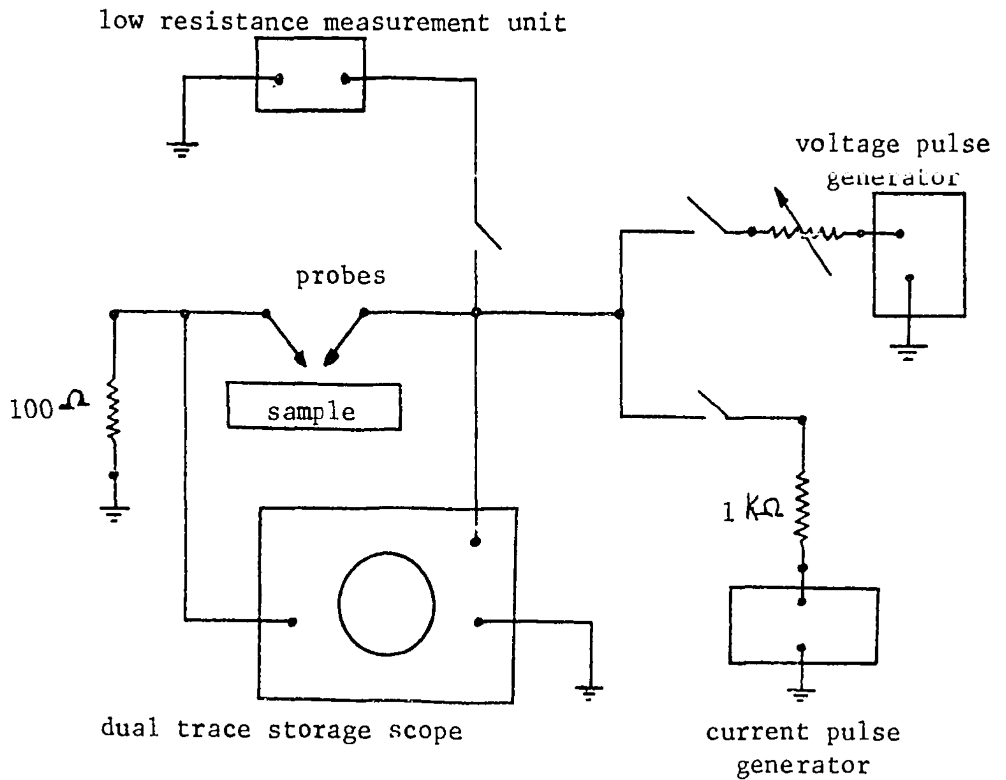

Figure 3. Experimental arrangement

is 1 microsecond. Two pulse generators and a low resistance measurement unit are isolated from each others in order to minimized parasitic capacitance.

In electron microprobe analysis a 20 kilovolts accelerating voltage is used with an absorbed electron current of 0.005 microamperes. The specimen is coated with a 100 A carbon film to provide a conducting path. A LiF crystal is used to detect As $L\alpha$ line, Te $L\alpha$ line, and Ge $K\alpha$ line. In each case the X-rays emitted from each element are counted for 20 seconds. The relative X-ray intensities are measured for the various elements at a spot in the center of the memory filament. By using a computer program, the atomic percentage of the filament composition can be determined.

A chemical etching process is needed to expose the cathode filament and to etch away the surface layer of the filament in order to examine its structure by electron scanning microscopy. Two kinds of chemical solutions are used:

1). 14 parts by volume of 49% HF, 10 parts by volume of 70% HNO_3, and 10 parts by volume of H_2O,

2). 17.8 gm of $Na_2Cr_2O_7$ crystals, 42.5 ml of 96.8% H_2SO_4, and 250 ml of H_2O.

The etching rate for both solutions is 8 um/min. The etching time used in this experiment is around one second. The etching process is performed at room temperature. The first etching solution exposes the cathode filament because of its uniform etching property. The second solution provides a good etching for electron scanning microscopy because it etchs along the

crystallization faces. The chemical solutions and etching rates are provided by Dr. C. H. Sie, ECD, Inc., Troy, Michigan.

A secondary emission mode is used in scanning electron microscopy to study specimen topography. Because the secondary electrons have low energies, they can be made to follow curved trajectories. As a result, holes or areas out of direct line of sight of collector will contain some detail. The secondary emission mode provides a remarkably detailed picture of the surface features of the specimen and depth of field. At 10,000X the depth of field is about 1 micrometer, and at 100X is about 1,000 micrometers. A 25 kilovolts accelerating voltage is used. The specimen is coated with a 100-200 A of gold-palladium alloy (Au 60%, Pd 40%) to provide a good conducting path.

C. Experimental Results

In this experiment the critical amplitude of the applied voltage to cause a breakdown is found to be about 160 volts. The corresponding critical field intensity will be calculated later. The experimental data of delay time and the associated applied voltage pulse are plotted on semi-logarithmic paper. It indicates that the relationship between the delay time and the amplitude of the applied voltage is an exponential function. The average value of the delay time and associated voltage are substituted in the simple exponential function:

$$t_d = A \exp (- BV). \tag{1}$$

Five equations are generated for V = 180, 220, 260, 300, and 340 volts.

Ratios of the nearest voltages are used to determine the two unknown constants. There are four values for the constant B, and five for the constant A. The average of these values leads to the following equation:

$$t_d = 4.37 \exp(-0.0171V) \qquad \text{sec.}, \qquad (2)$$

with V the amplitude of the applied voltage pulse in volts. Equation (2) and the experimental data are plotted in Figure 4.

It is found that there are two filaments in the memory switching process. One is initiated from the anode and the other from the cathode. The anode filament which is grown on the surface is wider than the cathode filament which is grown under the surface, as shown in Figure 5. The surface width of the anode filament is about 4 micrometers, and it is less than 3 micrometers for the cathode filament. The surface texture of both filaments is different.

The length of the memory switching time depends on how the connection is made between the filaments. A sudden voltage drop in the voltage characteristic curve of the filament formation corresponds to a connection between the anode and the cathode filaments, as shown in Figure 6. The voltage drop must be larger than 0.5 volts in less than 30 milliseconds. A smooth decreasing curve indicates a non-connection between the filaments as shown in Figure 7.

Since the filaments start to grow after the breakdown, the actual time it takes to grow a certain length of the filament is not the duration of the applied voltage pulse or the length of time from the application of the pulse until the voltage characteristic curve shows a sudden voltage drop. This is equal to the length of time from the application of the

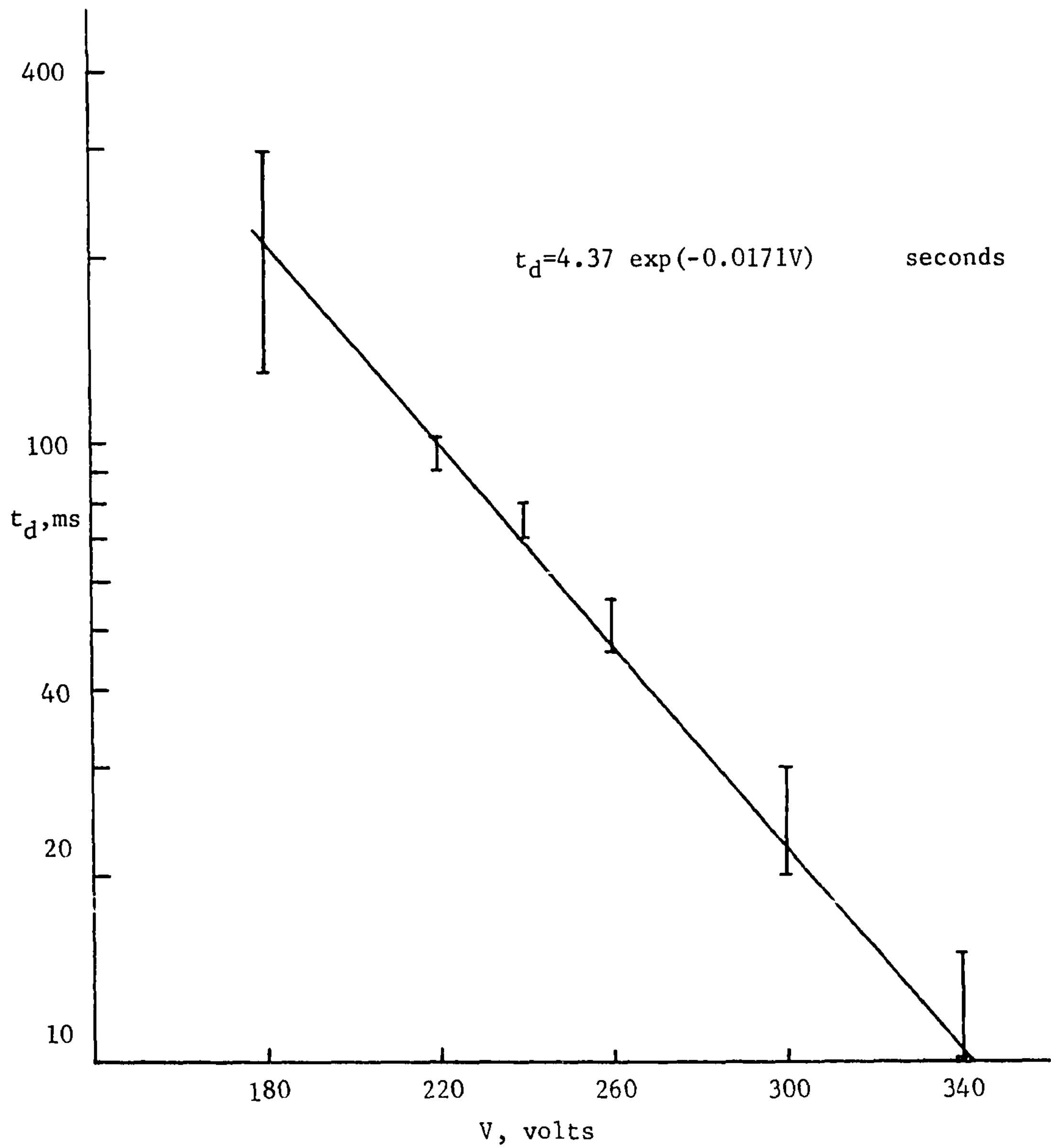

Figure 4. The relationship between the applied voltage and delay time (the equation $t_d = 4.37 \exp(-0.0171V)$ is only valid in the range between 180 to 340 volts)

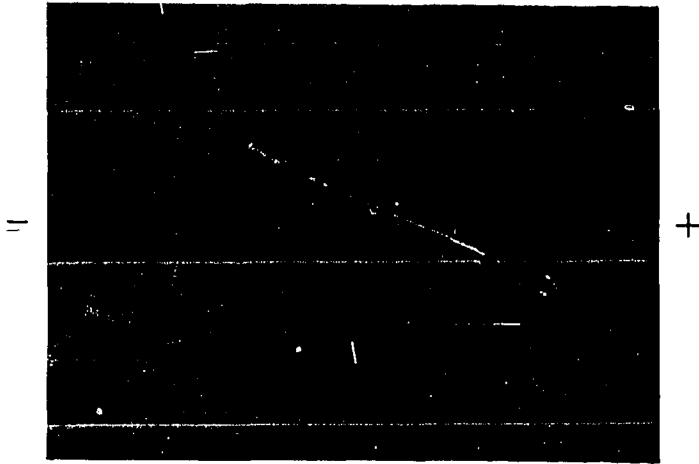

Figure 5a. The anode filament grown from the anode on the surface 526X

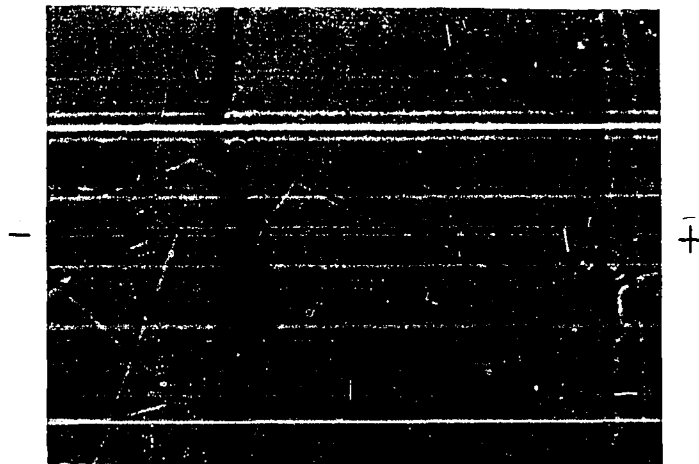

Figure 5b. The cathode filament appeared on the surface after etched in No. 1 chemical solution; same sample as 5a

Figure 6. The voltage drop in the voltage characteristic curve corresponds to a connection between the two filaments

6a. Voltage characteristic curve
Vertical scale: voltage 0.5 V/div.; current 0.5 ma/div.
Horizontal scale: 1 sec./div.

6b. Filamentary path 526X

6c. Same sample as 6b, etched in No. 1 chemical solution for 1 sec. 526X

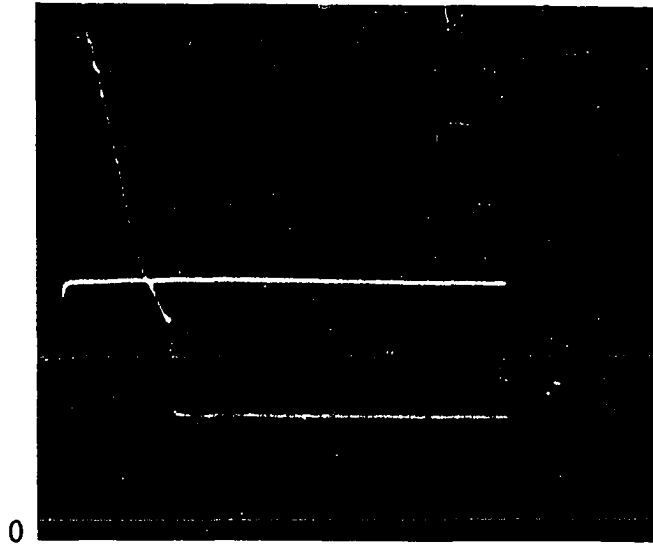
0

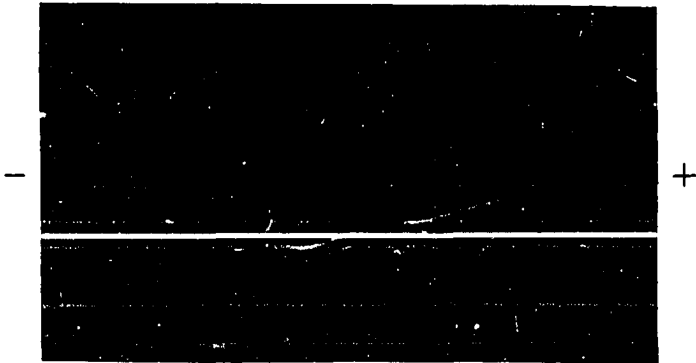
−
+

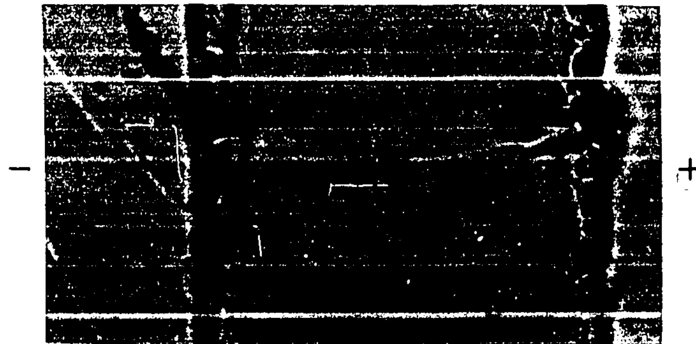
−
+

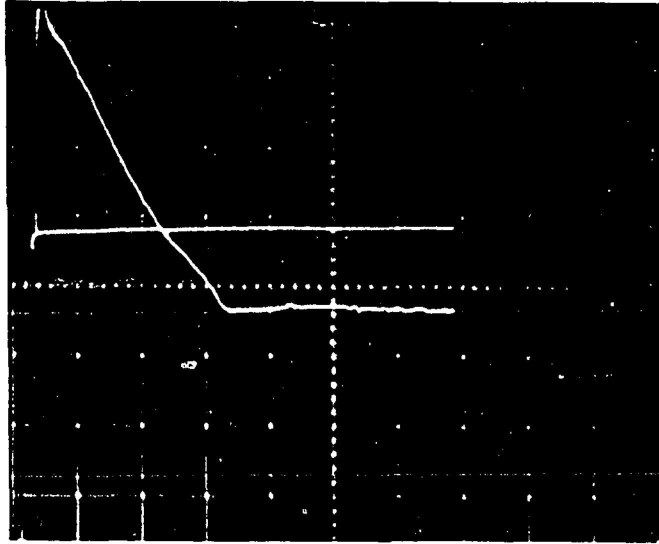

a. Voltage characteristic curve
Vertical scale: voltage 0.5 V/div.; current 0.5 ma/div.
Horizontal scale: 1 sec./div.

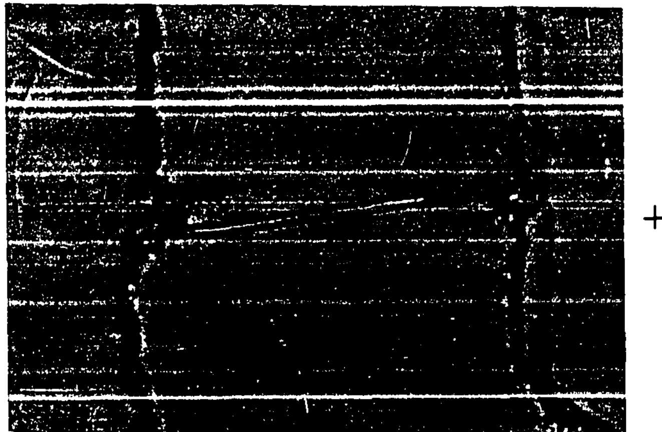

b. Filamentary path after etched in No. 1 chemical solution for 1 sec. 526X

Figure 7. No connection between two filaments with different surface texture; it is in low resistivity state

voltage pulse until a sudden voltage drop in the curve minus the delay time.

An optical microscope is used to measure the filament length. In this way the growth rate of the filaments can be calculated. The growth rate of the anode filament is faster than that of the cathode filament. However, the growth rate of the cathode filament can be improved by increasing the conducting current, as shown in Figure 8. The relation between the growth rate of the filaments and the conducting current is measured, as shown in Figure 9. The growth rate of the filaments is insensitive to the amplitude of the applied voltage pulse as expected.

Initially the resistance between the chromium electrodes is about 12-15 megohms. After switching from amorphous state to crystallized state, the resistance is about 400-600 ohms; on switching back from crystallized state to amorphous state, the resistance becomes between 5-8 megohms. In multiple switching the ratio between two states is about 10^4.

Both anode and cathode filament compositions are measured to be $As_{36}Te_{51}Ge_{13}$ as determined with an electron microprobe analyzer. For the experimental samples the measuring error is within ± 10%. This filament composition is located at the edge of the glass formation region in the As-Te-Ge phase diagram. The exothermic transition temperature is 300 deg. C., lower than that of the initial composition (6). It has a strong tendency to be crystallized. The topography of the etched filament is shown in Figure 10. The polycrystals are lined up because of the conducting current.

After the first cycle of the memory switching, continuous switching

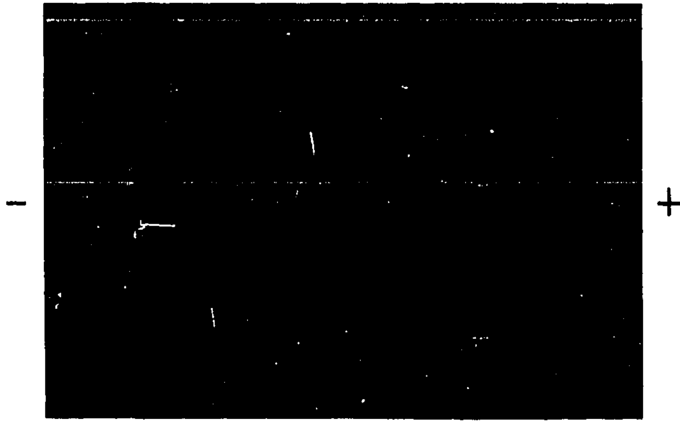

Figure 8. With 3.55 ma conducting current the growth rate of the cathode filament is increased; the sample was etched in No. 1 chemical solution 526X

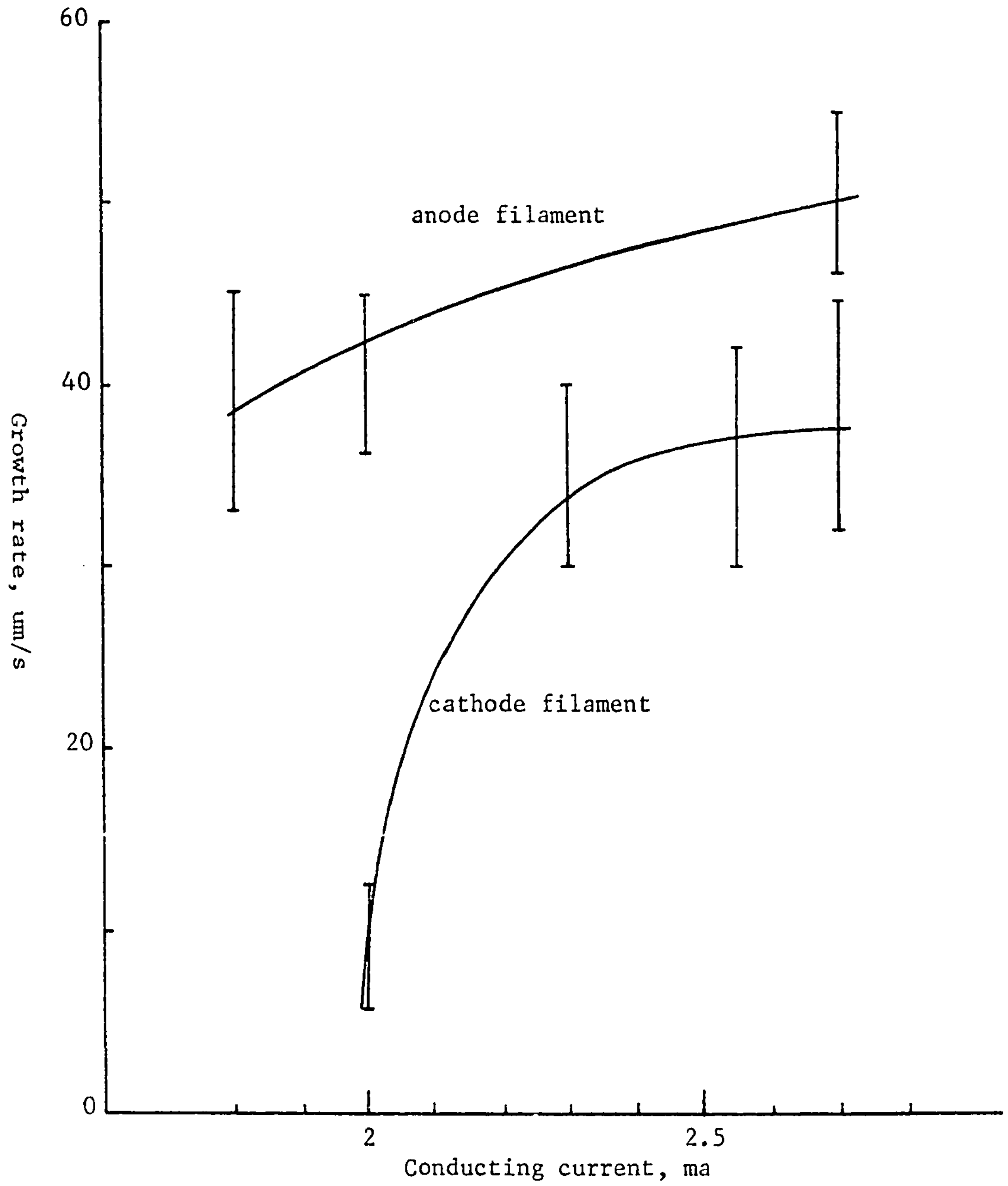

Figure 9. The average growth rate of the filaments

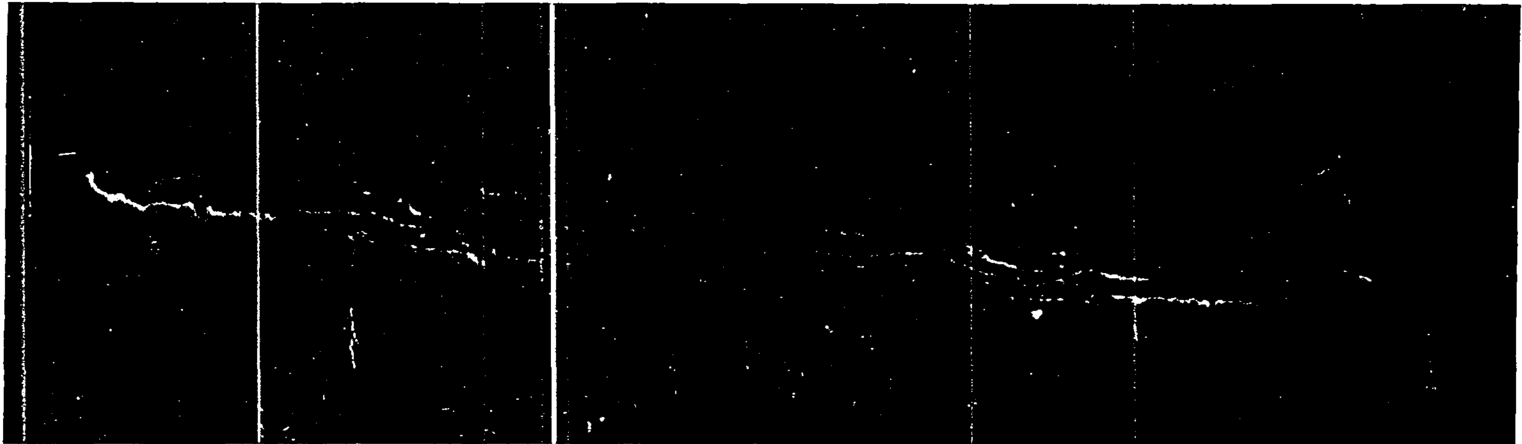

Figure 10. Topography of the memory filamentary path, etched with No. 2 chemical solution 1,700X

will reduce the amplitude of the applied voltage pulse needed for a memory switching. However, this may be due to temperature effects. Without any operation for a period of time, for example 20 minutes, the same amplitude of the applied voltage pulse is required for switching as was initially required.

IV. THEORY

A. The Basic Property of the Amorphous Chalcogenide

The amorphous chalcogenide is a kind of glass. The basic characteristics of a glass are shown in Figures 11, 12, after W. Kauzmann (21). There are two distingushing temperatures: a glass transition temperature T_g and a melting temperature T_m. With a slow cooling rate a liquid state glass will be cooled into a crystallized state. An amorphous state can only be obtained by a fast quenching process. An amorphous state is thermodynamically unstable, but a super-cooled liquid state is momentary thermodynamic equilibrium. Both are in metastable states relative to the stable crystallized state. A glass can stay in a metastable state indefinitely.

A super-cooled liquid can be crystallized at a certain temperature in between the glass transition temperature and the melting temperature as long as the characteristic curves of the rate of crystallization and the growth rate of crystals are properly overlapped (22). The rate of crystallization is zero at the melting temperature and rises to a maximum at lower temperature and falls back again to zero at absolute zero. The growth rate of crystals is negative at all temperature above the melting temperature and positive below the melting temperature. For most liquids the growth rate is very large at a temperature just below or very close to the melting temperature at which crystallization usually occurs. Foreign particles, structure defects, and local thermal fluctuations will favor the formation of nucleation centers of crystallization.

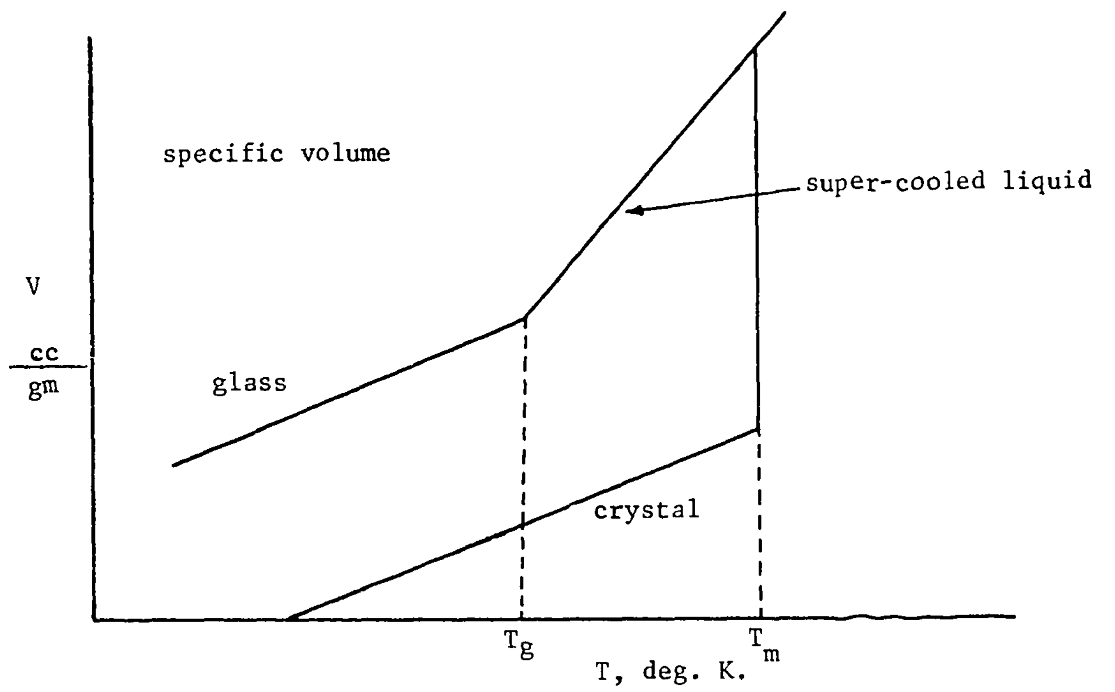

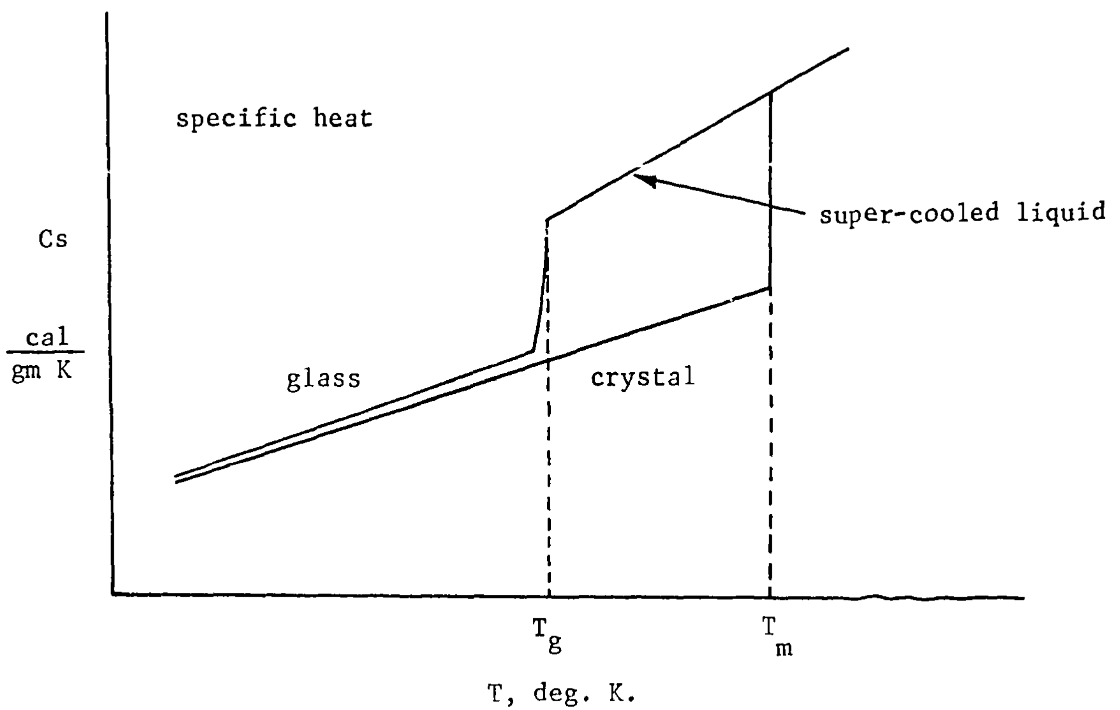

Figure 11. Thermodynamic properties of a glass (after Kauzmann)

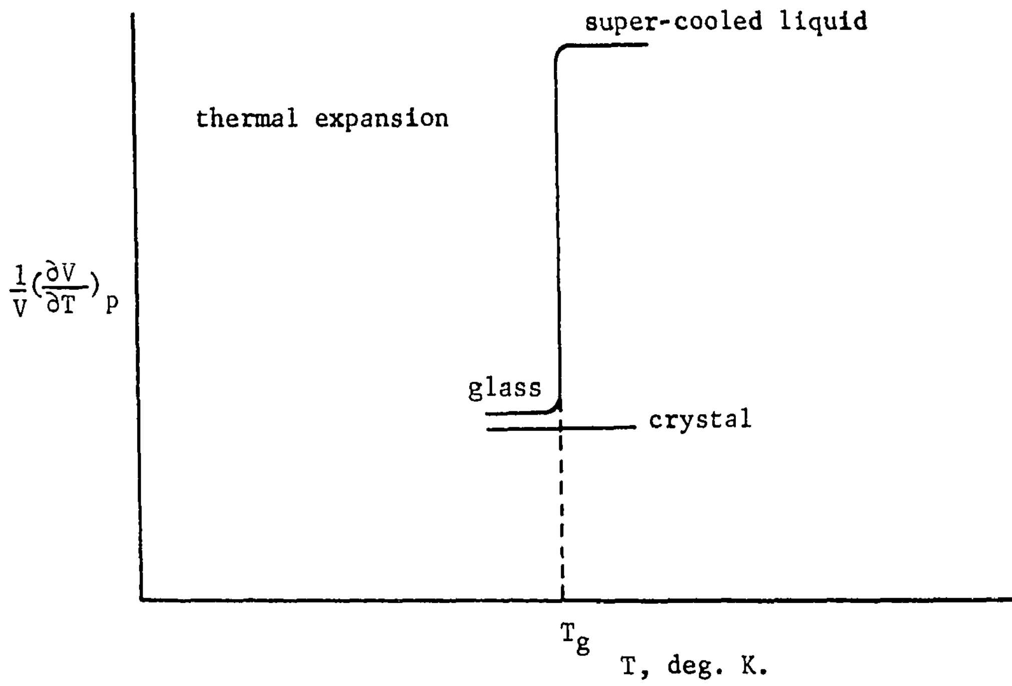

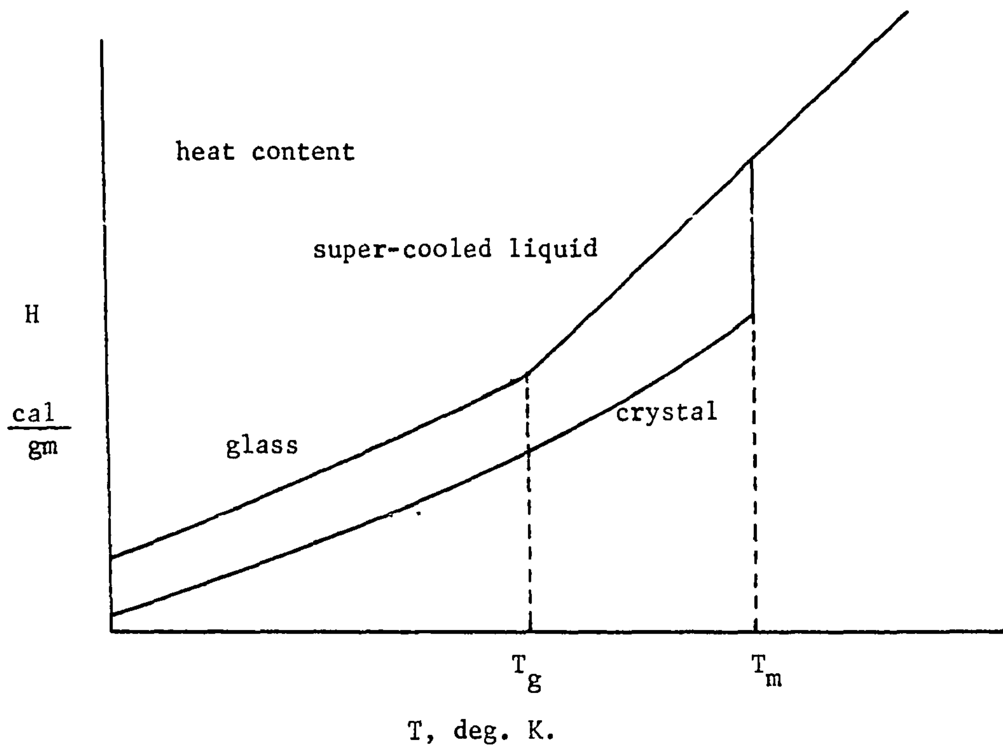

Figure 12. Thermodynamic properties of a glass (after Kauzmann)

By heating an amorphous chalcogenide or other amorphous materials, significant crystallization can occur in the super-cooled liquid state. This special temperature is called the exothermic transition temperature because the sudden change of the specific heat from a super-cooled liquid state to a crystallized state causes the release of its latent heat energy. The above idea has been confirmed by a differential thermal analysis for the amorphous chalcogenide which have a memory effect (15).

The electrical conductivity of the amorphous chalcogenide is a function of the activation energy, temperature, and the externally applied electric field. The activation energy varies in different temperature regions (23) for the amorphous chalcogenide as compared to this energy being nearly constant in highly ordered semiconductors. A constant activation energy is only expected to exist in a certain limited temperature range. It is higher in a high temperature region than in a low temperature region. For the high temperature region above 600 deg. K. the electrical conductivity can be represented by a linear relationship with temperature (6). The electric field inside the amorphous chalcogenide also plays an important role in determining the behavior of the electrical conductivity. The conductivity for the amorphous chalcogenide (17) can be expressed by

$$\sigma = \sigma_0 \exp\left[\xi/(CT) - \Delta E/(2kT)\right] \quad (3)$$

where σ_0 is a proportional constant in $ohm^{-1}cm^{-1}$,

ξ is the electric field intensity in V/cm,

ΔE is the energy gap in eV,

k is Boltzmann's constant in eV/deg. K.,

T is temperature in deg. K.,

C is a proportional constant in V/(cm deg. K).

The effective energy gap is reduced substantially by a high electric field. The effective energy gap is defined as

$$\Delta E' = \Delta E - 2k\xi/C. \quad (4)$$

However, the effect of the electric field and temperature dependance on the electrical conductivity is closely coupled and must be considered simultaneously. Naturally the specific heat is also a function of temperature.

A general breakdown is expected in all high resistivity materials with electrical stress. The amorphous chalcogenide materials are one class of high resistivity materials. However, the amorphous chalcogenide materials can be switched to a low resistivity state through a non-destructive breakdown. There are two kinds of breakdown involved: a thermal breakdown and an electronic breakdown. Most experimental data show that a thermal breakdown is a basic mechanism for the switching between two states for the amorphous chalcogenides and it is induced by an electric field (5, 18, 24). For a very thin film device the electronic mechanism could govern the breakdown process (5, 13). In a high electric field ($\gtrsim 10^5$ V/cm) there are many reported observations of breakdown in the amorphous chalcogenides (11, 19). Since the electrons gain energy from the applied field and their temperature is not allowed to be higher than the optical phonon temperature, it is expected that there will be a

strong energy transfer between the electrons and host lattices (11). The energy transfer results in a temperature increase to a critical value. Any local temperature increase above the critical value due to the local thermal fluctuation will cause a breakdown. However, the physical process which determines the property of the amorphous chalcogenide after breakdown has taken place, may be quite different from those which initiate and lead to a breakdown.

B. Critical Field Intensity and Breakdown Temperature

After the application of a voltage pulse across the electrodes, a non-uniform field is created between the electrodes in this special geometry, as shown in Figure 13. The field intensity is higher in the neighborhood of the electrodes. In order to calculate the field intensity between two electrodes, the following assumptions are made: the cross section of the end of the electrodes is assumed to be semicircular; half of the electrodes is buried into the amorphous chalcogenide; and fringing is eliminated by having the X and Y dimensions extend to infinity. Using conformal mapping technique, the field intensity can be expressed by

$$\xi(x) = 2V/[\pi d(1-x^2)^{1/2}] \qquad \text{V/cm} \qquad (5)$$

where V is the magnitude of the applied voltage pulse in volts,

d is the distance between two electrodes in cm,

x is a normalized parameter: x = 1 the geometrical center of the semicircular cross section of the end of positive electrode; x = -1 for that of the negative electrode.

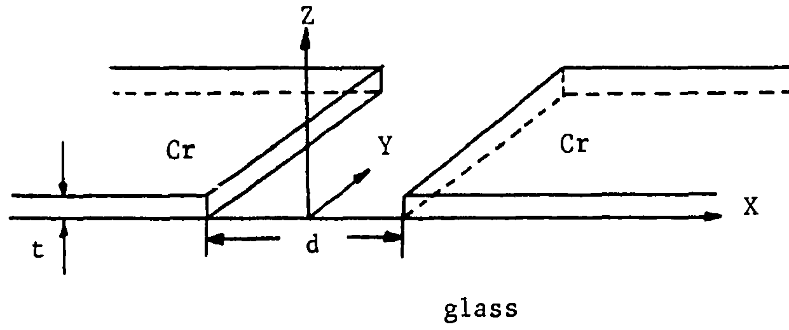

Figure 13a. The geometry of the device

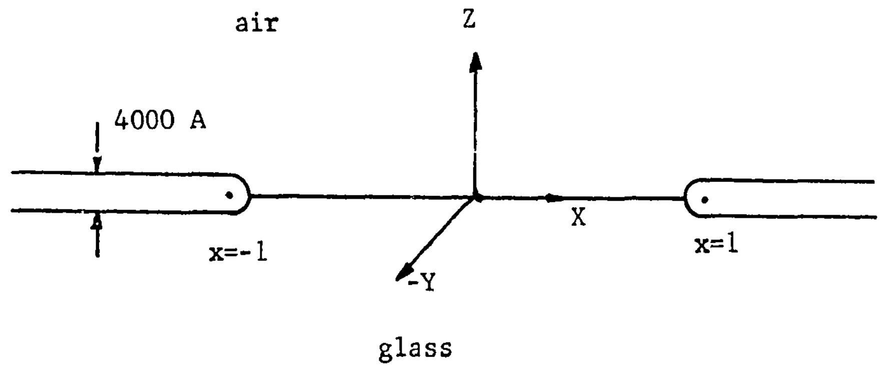

Figure 13b. A side view of a simplified geometry for field calculation

By substituting $x = 1 - t/(d)$ with $t = 4{,}000$ Å , the electrode thickness, the maximum field intensity near the electrodes is found to be

$$\xi_{max} = 707V \qquad V/cm. \tag{6}$$

The experimentally determined critical voltage of 160 volts corresponds to the critical field intensity

$$\xi_c = 1.13X10^5 \qquad V/cm$$

This field intensity is the same order of magnitude as the theoretical result reported by Hindley (11). Under this high field the electrons in amorphous chalcogenide are not in thermodynamical equilibrium with their host lattices. A strong energy transfer is expected from the interaction between hot electrons and optical phonons. Consequently, the temperature of the amorphous chalcogenide increases in the high field area.

Considering an infinitesimal volume of the amorphous chalcogenide for a thermal runaway, Warren and Male (17) found

$$\xi_c = C[-T_b^2/(T_b - T_o) + \Delta E/(2k)], \tag{7}$$

where T_b is the breakdown temperature for a thermal runaway in deg. K.,

T_o is the ambient temperature in deg. K.,

C is a proportional constant in V/(cm deg. K).

For a sandwich type sample with two perfect cooling electrodes, the critical applied voltage for a thermal breakdown can be calculated from the lattice energy balance equation

$$C_s\ \partial T/\partial t - \nabla\cdot K\,\nabla T = \sigma\xi^2 \qquad (8)$$

where C_s is specific heat per unit volume in J/cm^3 deg. K.,

K is the thermal conductivity in $W\ cm^{-1}\ K^{-1}$.

For a quasi-steady state thermal breakdown, the time derivative of temperature term can be omitted; the equation reads

$$\sigma\xi^2 + K\nabla^2 T = 0 \qquad (9)$$

assuming that K is independent of coordinates. Combined with the one dimension continuity equation

$$\nabla\cdot\sigma(-dV/dx\,\hat{i}) = 0\ , \qquad (10)$$

we have the critical applied voltage for a thermal breakdown:

$$V_c^2 = \frac{8kK}{\sigma_0[-k\xi_c/C + \Delta E/2]}\ \exp\left[\frac{-k\xi_c + \Delta E/2}{kT_0}\right] \qquad (11)$$

Substituting the critical field intensity into the above equation, we have

$$V_c^2\ x/(8KT_0) = \exp(x), \quad x = T_b^2/[T_0(T_b - T_0)]. \qquad (12)$$

Therefore, for the amorphous chalcogenide $As_{55}Te_{35}Ge_{10}$ in a sandwich type geometry, we get

$$T_b = 316 \text{ deg. K.},$$

by substituting $V_c = 1.13X10^3$ volts, $\Delta E = 1.12$ eV (6), $K = 5X10^{-3} W\ cm^{-1} K^{-1}$ (18), and $T_0 = 300$ deg. K. The equivalent applied voltage is estimated by multplying the maximum electric field intensity in the chromium electrodes

area with the distance between two electrodes on the surface of the bulk sample of the amorphous chalcogenide. This means that the breakdown temperature is only 16 deg. K above the room temperature. It is the same order of magnitude as the experimental data, 15-20 deg. K above the ambient, reported by Warren (18) and Stocker (25). This breakdown temperature is assumed to be valid for the material in the neighborhood of the electrodes for this experiment even though the geometry is different.

If the local temperature increases above the breakdown temperature in the high field area, then this will result in a thermal breakdown. Since the thermal runaway can only happen in a high field area and the propagation of the thermal runaway follows the field lines (25), the material involved in the thermal breakdown is limited. After the thermal breakdown the stored energy in the parasitic capacitor discharges into the breakdown channel. The energy balance equation is expressed by

$$C_s A d(T - T_b) = C'V^2/2 + \int_{t_s} IVdt, \qquad (13)$$

where C' is parasitic capacitor between the electrodes in farads,

A is the cross section of the amorphous chalcogenide which is involved in the absorption of joule self-heating in cm^2,

t_s is switching time in seconds which is the time that elapses from the moment of increasing conducting current to the time when the current is saturated,

I is conducting current in amperes,

C_s is specific heat per unit volume in J/cm^3 deg. K.

The electrical conductivity for the amorphous chalcogenide $As_{55}Te_{35}Ge_{10}$ in a high temperature region can be expressed by (6)

$$\sigma = 10^{(8620T - 5.44X10^6)/T^2} \quad ohm^{-1}cm^{-1}. \tag{14}$$

We have

$$T = 1750 \text{ deg. K}, \tag{15}$$

by substituting $A = d/(\sigma R)$, $V = 160$ volts, $C' = 10^{-11}$ farads, $C_s = 1J/cm^3K$ (5, 18), $R = 10^3$ ohm, $d = 10^{-2}$ cm, and $T_b = 316$ deg. K. With this high local temperature, a vapor cloud (14) and melting phenomena is observed in every initial switching. The thermal diffusion in the radial direction and heat radiation provide a heat sink for the local high temperature region.

For a sandwich type chalcogenide device, the thermal diffusion in the radial direction after thermal breakdown can be described by the diffusion equation in cyclinder coordinate. Assuming that the temperature distribution at the center of the device is only dependent on the radius r, the diffusion equation reads

$$\nabla^2 T = \frac{\partial^2 T}{\partial r^2} + \frac{\partial T}{r\partial r} = \frac{1}{c^2}\frac{\partial T}{\partial t}, \quad c^2 = K/C_s. \tag{16}$$

By using Laplace transformation and countour integration in complex plane, we have

$$T(r,t) = T(r,0) + \frac{2T(r,0)}{\pi}\int_0^\infty e^{-tu^2}\left[\frac{J_o(ru/c)Y_o(au/c)-Y_o(ru/c)J_o(au/c)}{J_o^2(au/c)+Y_o^2(au/c)}\right]\frac{du}{u}, \tag{17}$$

where $T(r,0)$ = constant is initial temperature distribution, $0 \le r \le a$,

J_o is the zero order Bessel function of first kind,

Y_o is the zero order Bessel function of second kind.

The above equation can only be solved by numerical methods. For the geometry used in this experiment, the diffusion equation also has to be solved by numerical methods. In order to estimate the thermal wave propagation on the surface in the surface switching, the one-dimension diffusion equation is used:

$$\frac{\partial^2 T}{\partial y^2} = \frac{1}{c^2} \frac{\partial T}{\partial t} . \tag{18}$$

The solution is

$$T(y,t) = \frac{1}{2c\sqrt{\pi t}} \int_{\infty}^{\infty} f(v) \exp\left[\frac{-(y-v)^2}{4c^2 t}\right] dv, \tag{19}$$

where $f(v)$ is initial temperature distribution.

Assuming the initial heat source is a step function, we have

$$T(y,t) = \frac{T(y,0)}{2} \left[-\operatorname{erf}\left(\frac{y-a}{2c^2\sqrt{t}}\right) + \operatorname{erf}\left(\frac{y+a}{2c^2\sqrt{t}}\right)\right]. \tag{20}$$

where

$T(y,0)$, $0 \le y \le a$, is initial temperature distribution,

erf is the error function.

In this experiment, the radius, a, of the initial temperature source is about 2um. From equation (15) we have the initial source of temperature above the ambient temperature:

$$T_o = 1750 - 300 = 1450^o$$

The propagation constant of the amorphous chalcogenide $As_{55}Te_{35}Ge_{10}$ is

$$c^2 = 5X10^{-3}cm^2/sec.$$

Five microseconds after breakdown, the melt region has grown five micrometers away from the center of the heat source. This result is of the same order of magnitude as the experimental data, about 6-8 micrometers.

C. Voltage Characteristic Curve of Filament Formation

The voltage characteristic curve of filament formation as shown in Fig. 6a provides some information of the filament formation process. It can be divided into three periods of time: delay time period, filament formation period, and low resistivity state period. The applied high voltage pulse creates a very high electric field intensity near the electrodes. Any local temperature increase above the breakdown temperature will lead to a breakdown. A period of time in which a breakdown occurs after the application of a high voltage pulse across the electrodes is defined as a delay time. After the breakdown a dynamic low resistivity of the chalcogenide is formed between the electrodes. In addition to the heat radiation to the air and a thermal cooling through the electrodes, there is also the thermal diffusion that takes place along the radial direction. Both melting and thermal diffusion can be observed through an optical microscope during a breakdown period. At the same time the memory filaments start to grow from both electrodes along the boundary region of the dynamic low

resistivity channel. This is the time at which the filament formation period starts. The growth rate of the filament growing from the anode is relatively constant and faster than that of the cathode filament. At 1.8 ma conducting current the average growth rate for the anode filament growth rate is smaller and subject to large error due to it being near the limit of measurability of the technique used. At 2.3 ma conducting current, the growth rate is about 44 um/sec. for the anode filament and 35 um/sec. for the cathode filament. It is difficult to observe the cathode filament because it always grows under the surface in this geometry. The reason may be due to the small cross section of the cathode filament and its field direction dependence. The maximum field at the electrodes is pointed downward instead of being parallel to the surface because of the device structure. Once the filament starts to grow, it will tend to follow a contour line in which significant crystallization will occur. The region in which these contour lines lie will be described in detail later. After the completion of the formation of the memory filament, the cell stay in a low resistivity state without excitation. If the voltage pulse terminates before the completion of the memory filament, then the resistance between the electrodes will remain at a high value after excitation removed and time of recovery (26). This situation is quite different from a threshold chalcogenide semiconductor which provides a dynamic low resistivity path only for the duration of the applied voltage and recovery. For the memory chalcogenide semiconductors incompleted low resistivity filaments can be grown as shown in Fig. 14. The only possible way to complete a memory switching is that the duration of the applied voltage pulse is long enough

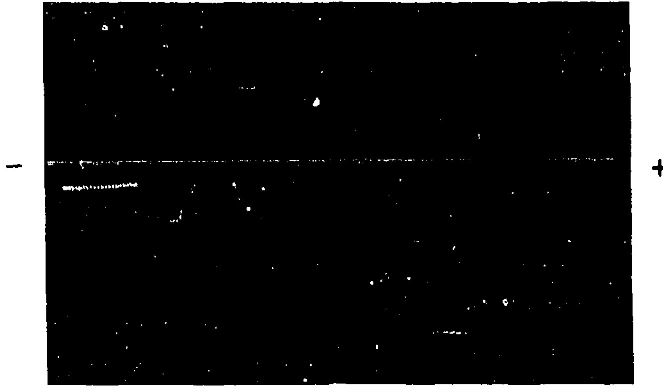

Figure 14. No connection between the two filaments, in high resistance state 526X

such that the memory filament can be completed. The duration must be equal to or longer than the delay time plus filament growing time. Using 180 volts pulse with 1.8 ma conducting current in this experiment, the duration of the applied pulse needed for a memory switching is about 2-3 seconds. Applying the same magnitude of the pulse with 2.3 ma conducting current, it needs about 1.5 seconds duration pulse to complete a memory switching.

From the top view of the sample surface, the temperature distribution between the electrodes can be divided into three different regions at the moment of breakdown: center melt region (a dynamic low resistivity channel), glass transition to melting temperature region, and below glass transition temperature region. The thermal differential analysis indicates that the amorphous chalcogenide for a memory effect will release its latent thermal energy when passing through its exothermic transition temperature, and will start to crystallize. The exothermic transition temperature is always below the melting temperature. In the center melt region the crystallization cannot exist due to the high temperature. However, it provides a dynamic low resistivity path for the duration of the applied voltage pulse, even if the filament never grows. The crystallization can only be found in some areas of the glass transition and melting temperature region. It depends on joule self-heating, thermal diffusion, and thermal sinks. There is a semi-cone area where the filaments can be grown.

During the redistribution of the conducting current because of the growth of the memory filaments, a portion of the dynamic low resistivity channel will quench into an amorphous state as shown in Fig. 15. A fast

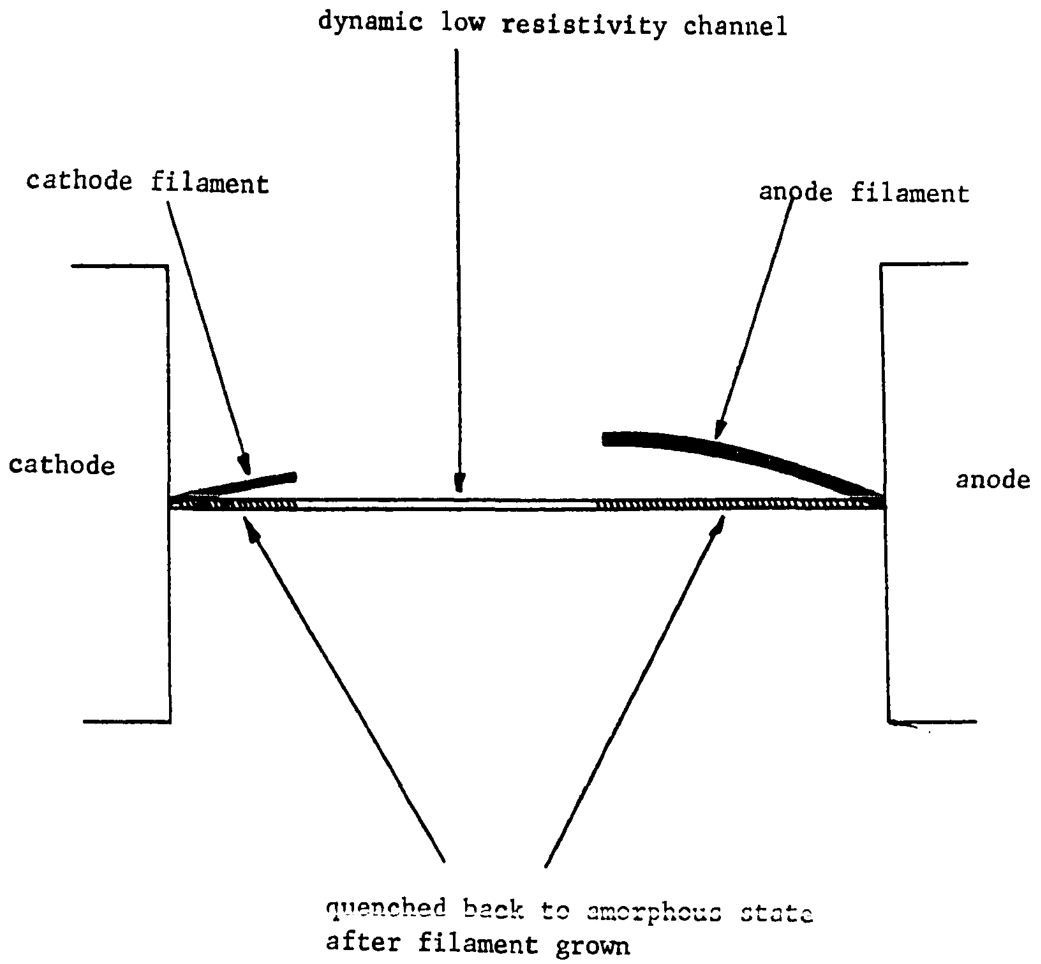

Figure 15. Top view of the device during the filament formation

cooling rate is needed for this process. As long as the conducting current is not large enough to heat up locally any portion of the memory filament above its melting temperature, the memory filament will quench into a crystallization state independent of the cooling rate.

Breakdown causes the material between the electrodes to be elevated to a high temperature above the ambient. The temperature increase results from joule self-heating provided by the conducting current. For a surface switching device, this high temperature above the exothermic transition temperature is maintained until the growing filament passes through the spot where the temperature is being monitored with a radiometric microscope. The filament temperature is only slightly higher than the ambient temperature as reported by Sie (16). This also implies that the memory filament is in a low resistivity state because the joule self-heating is less and the filament is a good thermal conducting path. For a sandwich type device, the variation of temperature and conducting current density at various times after applying an electric field were studied by Warren (18), as shown in Fig. 16. It is seen that there is very little change in either the temperature or the conducting current density during a large delay time (about 2 ms in this case). If the field is less than the critical field, the temperature distribution attains equilibrium with a center temperature less than the critical breakdown temperature ($320^{o}K$ in this case) and hence, no breakdown is observed. After breakdown a dynamic low resistivity channel will form and crystallization will occur in between the center melt channel and the above exothermic transition temperature region. Under a slow

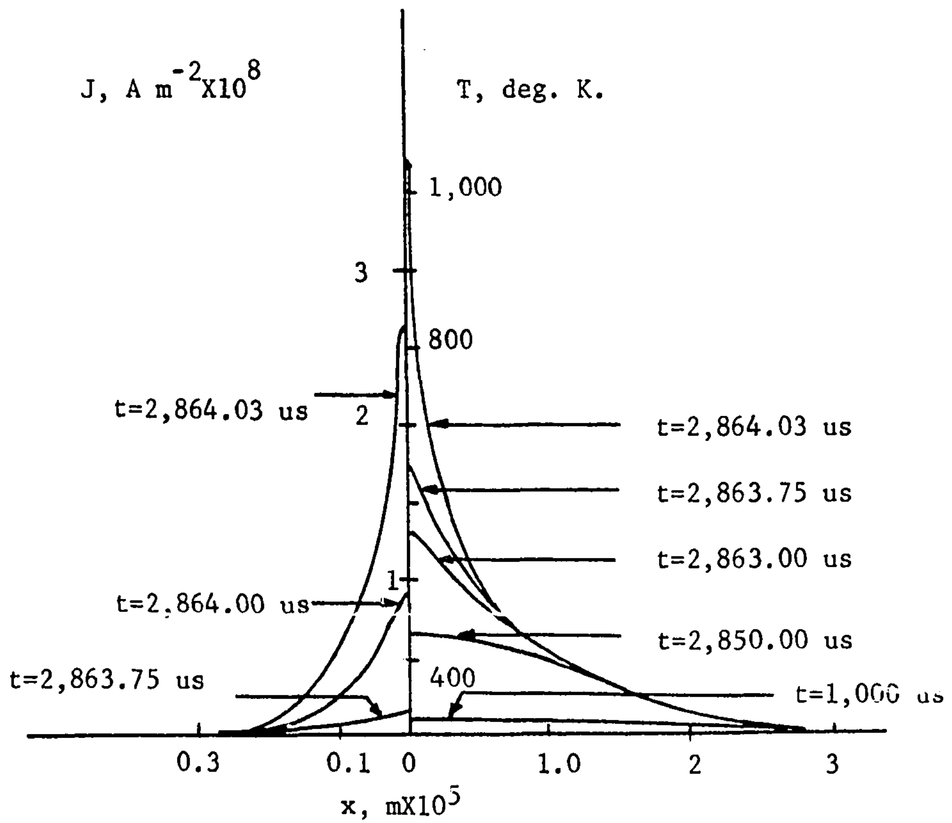

Figure 16. Temperature and current density within slab at various times after the application of electric field $5.9X10^5$ V/cm (after Warren)

cooling rate the center melt channel will also quench into a crystallization state.

D. Connection Between the Anode and the Cathode Filaments

The connection method for the filaments growing from the anode and the cathode has a significant effect on the variation in the time needed to complete a memory switching. If both filaments are growing along the same contour curve on the same side of the center melt region, it will be one of the optimum ways to connect the two filaments in the shortest time. For a non-direct connection between the two filaments, it will take a longer time to complete a memory switching. Both cases indicate themselves clearly in the voltage characteristic curve of the memory filament formation. The first sudden voltage drop in the curve corresponds to a direct connection between the filaments as shown in Fig 6.

A filament that grows between the anode filament and the cathode filament must bypass the dynamic low resistivity channel. If a filament traverses the dynamic low resistivity channel, it needs a slow cooling rate to quench the section of the channel into a crystallization state and the quenching process has to be completed before the termination of excitation. Otherwise, it will quench into an amorphous state or a partial crystallization state. Thermodynamically, this is not a possible connection.

If the path between the two filaments provides a higher resistance than that between the anode filament and the cathode, the anode and the cathode filament will not connect together. The lowest resistance path between the anode filament and the cathode results from the polycrystal-

lization presented along the transition boundary. However, the energy gap in the crystal boundary may be large (8) and the polycrystallization path may present a higher resistance path than a small section of the dynamic low resistivity channel.

Without any sudden voltage drop but with a smooth decreasing curve, it shall belong to the non-direct connection of the two filaments, as shown in Figure 7. Two voltage drops in the curve indicates two connections between the filaments as shown in Figure 17. The magnitude of a second voltage drop is about 0.3-0.1 volts.

E. Growth Rate of the Filaments

The growth rate of the anode filament is relatively constant compared with that of the cathode filament. At a low conducting current level the growth rate of the cathode filament is small and subjects to a large error due to the measuring technique used. These two types of filaments are distinguishable because they have different surface textures after chemical etching process. The maximum memory switching time can be estimated by the growth rate of the anode filament. However, through the control of the growth of the cathode filament both its rate and position will provide a good opportunity to reduce the memory switching time substantially. The precise location of the filamentary path is sensitive to local inhomogeneity since these give rise to high field points. The filaments have a tendency to grow near the center melt region as the conducting current is increased. The growth rate of the cathode filament can also be improved by increasing the conducting current level.

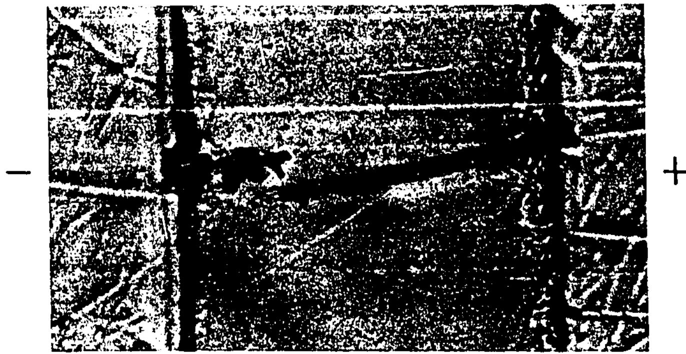

Figure 17. Two connections between the two filaments, etched with No. 1 chemical solution for 1 sec. 526X

Utilizing the relationship between the growth rate of the filaments and the conducting current level, one can find an optimum conducting current to operate the amorphous chalcogenide device to have a fast and secure switching. In estimating an optimum conducting current, one has to consider the saturation of the growth rate, thermal sinks in the electrodes, and the property of the electrode material.

It is found that the optimum conducting current in this experiment is about 2.3 ma. At this conducting current level the growth rate of the cathode filament tends to saturate and the growth rate is about 35 um/sec. The average memory switching time is about 1.5-2 sec. with 180 volts applied voltage pulse.

V. CONCLUSION

The preceding pages have presented a series of observation of the memory switching properties in the surface of bulk samples of the amorphous chalcogenide $As_{55}Te_{35}Ge_{10}$ with chromium electrodes. There are two filaments, one initiated from the anode and the other from the cathode. The average growth rate of the filaments has a tendency to saturate when increasing the conducting current level. The optimum conducting current can be chosen such that a fast and secure memory switching will be achieved. In doing so the thermal property of the electrodes has to be considered in order to have an adequate fast quenching rate in the junction between the electrodes and the memory filament. Without a good effective thermal sink in the electrodes, the device made from the amorphous chalcogenide can not be a switchable memory device. In addition, the material of the electrodes has to have a high melting point and a low diffusion coefficient. An electrode material with a high diffusion coefficient will result in a short circuit in the device after several switching cycles.

The voltage characteristic curve of the filament formation provides some basic information of the filament formation process. A sudden voltage drop in the curve corresponds to a direct connection between the filaments. Without a direct connection between the filaments, the memory switching time will be increased and the voltage characteristic curve will indicate this by a smoothly decreasing curve.

The growth rate of the filaments is a function of the conducting current and for a large current the growth rate saturates. To achieve

fast switching the growth rate must be maximized. For large conducting currents the electrodes and the surface are adversely affected so the conducting current required is that at which the growth rate just saturates. With such a high conducting current the filamentary path tends to grow along the center melt region which is defined at the moment of breakdown. This condition leads to a very high probability to have a direct connection between the filaments. The manner of connection between the filaments is the dominating factor in determining the length of the memory switching time.

Two types of filaments are distinguishable because they have different surface textures after chemical etching. The growth rate of the cathode filament is uncertain at low conducting current levels. In addition, the cathode filament is grown under the surface and the anode filament on the surface. These indicates that there are two different physical processes involved in forming a filamentary path. It is believed that the anode filament formation is dependent on ion motion. The cathode filament formation is unexplained at this time but it may be dependent on electron motion.

The memory filament starts to grow after the breakdown which is initiated by a high electric field. During the formation of a memory filament, the electric field is low across the electrodes while the conducting current is constant. The conducting current provides the necessary joule heating energy required to maintain the temperature of the material between the electrodes above the exothermic transition temperature. The thermal differential analysis shows that there is an exothermic

transition temperature in the amorphous chalcogenides for a memory effect. A memory effect of the amorphous chalcogenides involves a transition between two different structures, and this occurs above the exothermic transition temperature.

VI. BIBLIOGRAPHY

1. Pearson, A. D., Northover, W. R., Dewald, J. F., and Peck, W. F. Jr. Chemical, physical, and electrical properties of some unusual inorganic glasses. In Advance in Glass Technology. Pp 357-365. New York, New York, Plenum Press. 1962.

2. Ovshinsky, S. R. Reversible electrical switching phenomena in disordered structures. Phys. Rev. Lett. 21: 1450-1453. 1968.

3. Sie, C. H. A memory cell using bulk effect in amorphous semiconductor. Unpublished paper presented at the Sixth Annual Report, Affiliate Program in Solid-State Electronics, Iowa State University, Ames, Iowa, May 22, 1968. Ames, Iowa, Research Inst., Iowa State University. 1968.

4. Uttecht, R. R., Stevenson, H., Sie, C. H., Griener, J. D., and Raghavan, K. S. Electric field-induced filament formation in As-Te-Ge glass. J. of Non-cry. Solids 2: 358-370. 1970.

5. Fritzsche, H. and Ovshinsky, S. R. Conduction and switching phenomena in covalent alloy semiconductors. J. of Non-cry. Solids 4: 464-479. 1970.

6. Krebs, H. and Fischer, P. Electrical conductivity of melts and their ability to form glasses in the system Ge-As-Te. Faraday Soc. Discussions 50: 35-44. 1970.

7. Mott, N. F. Metal-insulator transition. Rev. Mod. Phys. 40: 677-683. 1968.

8. Mott, N. F. Electrons in disordered structures. Adv. in Phys. 16, No. 61: 49-144. 1967.

9. Cohen, M. H., Fritzsche, H., and Ovshinsky, S. R. Simple band model for amorphous semiconducting alloys. Phys. Rev. Lett. 22: 1065-1068. 1969.

10. Mott, N. F. Conduction in non-crystalline systems: Localized electronic states in disordered systems. Phil. Mag. 17: 1259-1268. 1968.

11. Hindley, N. K. Random phase model of amorphous semiconductors. J. of Non-crys. Solids 2: 432-443. 1970.

12. Boer, K. W. The conduction mechanism of self-compensated highly disordered semiconductors. Phys. Stat. Sol. 34: 721-739. 1969.

13. Mattis, D. C. Theory of electronic switching effect as a coopera-

tive phenomenon. Phys. Rev. Lett. 22, No. 18: 936-939. 1969.

14. Johnson, R. T., Northrop, D. A., and Quinn, R. K. Vaporization associated with surface electrical switching in semiconducting As-Te-I and As-Te-Ge glasses. Solid State Comm. 9, No. 16: 1397-1401. 1971.

15. Fritzsche, H. and Ovshinsky, S. R. Calorimetric and dilatometric studies on chalcogenide alloy glasses. J. of Non-crys. Solids 2: 148-154. 1970.

16. Sie, C. H. Electron microprobe analysis and radiometric microscopy of electric field induced filament formation on the surface of As-Te-Ge glass. J. of Non-crys. Solids 4: 548-553. 1970.

17. Warren, A. C. and Male, J. C. Field-enhanced conductivity effects in thin chalcogenide-glass switches. Elec. Lett. 6, No. 18: 567-569. 1970.

18. Warren, A. C. Switching mechanism in chalcogenide glasses. Elec. Lett. 5, No. 19: 461-462. 1969.

19. Kolomiets, V. T., Lebedev, E. A., and Taksami, I. A. Principal parameters of switches based on glassy chalcogenide semiconductors. Soviet Phys. Semi. 3, No. 5: 621-624. 1969.

20. Hilton, A. R., Jones, C. E., and Brau, M. Non-oxide IVA-VA-VIA chalcogenide glasses. Part 1. Glass-forming regions and variations in physical properties. Phys. and Chem. of Glasses 7, No. 4: 105-112. 1966.

21. Kauzmann, W. The nature of the glassy state and the behavior of liquids at low temperatures. Chem. Rev. 43: 219-256. 1948.

22. Jones, G. O. Glass. New York, New York, John Wiley and Sons Inc. 1956.

23. Male, J. C. Conductivity of electrical switching chalcogenide glass. Elec. Lett. 6, No. 4: 91-92. 1970.

24. Ridley, B. K. Specific negative resistance in solids. Proc. Phys. Soc. (London) 82: 954-966. 1963.

25. Stocker, H. J. Phenomenology of switching and memory effects in semiconducting chalcogenide glasses. J. of Non-crys. Solids 2: 371-381. 1970.

26. Shanks, R. R. Ovonic threshold switching characteristics. J. of Non-crys. Solids 2: 504-514. 1970.

VII. ACKNOWLEDGEMENTS

The writer wished to offer his sincere thanks to Professor A. V. Pohm of the Department of Electrical Engineering, Iowa State University, for suggesting this area of research and his criticism of this manuscript. He also wishes to thank Dr. C. H. Sie, Energy Devices Conversion, Inc., Michigan, for providing the chemical etching solutions.

The writer gratefully acknowledges the financial support given by the Solid State Affiliate Program of the Engineering Research Institute, Iowa State University.

And the writer wishes to thank his wife, without whose patience and encouragement this manuscript would not have been possible.